

Vibrational Spectral Studies and Electronics Properties of Non-Linear Optical Heterocyclic Compound 3-Amino Pyrazole - DFT Study

Sushma Priya Y¹, Ramachandra Rao K², Venkata Chalapathi P³ and Veeraiah A^{4*}

¹Department of Physics, Adikavi Nannaya University, India

²Department of Physics, Government College (A), India

³Department of Physics, Jawaharlal Nehru Technological University Kakinada, India

⁴Department of Physics, DNR College (A), India

Volume 1 Issue 3- 2018

Received Date: 01 Oct 2018

Accepted Date: 25 Oct 2018

Published Date: 30 Oct 2018

2. Key words

3-Amino pyrazole; DFT; FT-IR; FT-RAMAN; UV-V is Spectrum; NBO; HOMO and LUMO

1. Abstract

3-Amino Pyrazole (3AP) is used as the remedial agent for the cure of cancer and cell proliferative disorders. In the present communication vibrational frequencies and the structural properties of 3AP have been investigated using Density Functional Theory (DFT) employing B3LYP exchange-correlation with high level basis set 6-311++G (d, p). The FT-IR Liquid phase (4000-400cm⁻¹) and FT-Raman spectra (4000-400cm⁻¹) of 3AP was recorded at room temperature. By following the Scaled Quantum Mechanical Force Field method (SQMFF) the task of assigning the vibrational spectra by means of Normal Coordinate Analysis (NCA) was obtained and compared with experimental FT-IR and FT-Raman spectra. The NLO properties of 3AP have been computed using quantum mechanical calculations. The Natural Bond Orbital and HOMO, LUMO analysis has also been carried out for the title compound. Thermal properties of 3AP at different temperatures have been calculated on the basis of vibrational analysis. UV-visible spectrum of the compound was recorded in the region 200-800 nm.

3. Introduction

Pyrazole refers to a 5-membered Heterocyclic compound distinguished through three carbon atoms and two adjacent nitrogen atoms. In recent years Pyrazoles have attracted the interest of researchers in the field of medicine and agriculture. Pyrazole is a biologically active compound having the wide range of applications in pharmacological industries such as anti-inflammatory [1], antitumor [2], anticonvulsant [3], antidepressant [4] and antimicrobial [5,6] activities. It is also found Pyrazoles have widespread applications in the fields of supramolecular chemistry, crystal engineering, material sciences, sensors, biochemistry, catalysis etc. [7-14]. Pyrazole derivatives are well known fluorescent compounds with high quantum yields and are used as optical brightening agents for textiles, fabrics, plastics and papers. There have been several studies reported [15-17] for the vibrational analysis of pyrazole.

Recently Meryem Evecen et al. [18] was reported theoretical investigations on 1-(2-nitrobenzoyl) 3, 5-bis (4-methoxyph-

nyl)-4, 5-dihydro-¹H-pyrazole. Vibrational spectral studies of 3, 5-dimethyl pyrazole based on density functional calculations have been done by Krishna kumar et al. [19]. Literature investigation specifies there is no absolute study of both experimental and theoretical study of 3AP compound. In the present study, we have elucidated the optimized geometrical parameters, different normal modes of 3AP. The vibrational frequencies of the compound 3AP are allotted to normal modes based on Potential Energy Distribution (PED). By Natural Bonding Orbital (NBO) analysis hyper conjugative interaction and Intermolecular Charge Transfers (ICT) are interpreted. The first order hyperpolarizability, dipole moment, HOMO and LUMO Energies of 3AP are calculated using DFT/B3LYP method using 6-311++G** basis set. Different thermodynamic properties were theoretically calculated using harmonic vibrations.

4. Experimental Details

The liquid sample of commercially available 3-Aminopyrazole was procured from sigma Aldrich chemical company (USA)

*Corresponding Author (s): Veeraiah A, Department of Physics, DNR College (A), Bhimavaram, India, E-mail: avru@rediffmail.com

was used as such in the spectroscopic investigations. Fourier transform-infrared spectra (FT-IR) of 3AP was recorded using KBr pellet method in the region 400–4000 cm^{-1} using a Nicolet 6700 FTIR spectrometer at a resolution of $\pm 1 \text{ cm}^{-1}$ with UV or visible laser excitation with a Thermo Nicolet Continuum IR microscope. FT-Raman spectrum of the 3AP with a Nicolet Magna 750 Raman spectrometer at a resolution of 4 cm^{-1} in spectrum range (Stokes region) 4000–50 cm^{-1} using the 1064 nm line of an Nd: YAG laser for excitation operating at 500 mW Power operated with an InGaAs (Indium gallium arsenide) detector. UV-Vis spectrum of the compound has been using a Perkin Elmer Lambda 35 UV-Vis spectrometer. All the data were recorded after 1 cycle, with a Period of 1 nm slit width of 2 nm and a scan rate of $240 \text{ nm} \cdot \text{min}^{-1}$ with the spectral resolution of 0.05 – 4.0 nm. The UV-V is spectrum was recorded using dimethyl sulphuric acid as solvent.

4.1. Computational details

Density functional computations were carried out using Gaussian 09 W Revision- A.02 SMP [20] using Becke's Three-Parameter (B3LYP) hybrid DFT level applied with the typical 6-311++G** basis set to optimize the molecular geometry. The harmonic vibrational frequencies were calculated by taking the second order derivative of the energy and the predicted frequencies were scaled according to Scaled Quantum Mechanical (SQM) procedure [21-23] followed by the Potential Energy Distribution (PED) matrix. The characterization of the normal modes of 3AP was carried out through with the MOLVIB -7.0 Program using Potential Energy Distribution (PED) written by Sundius [24,25]. In order to know the intra-molecular delocalization or hyper conjugation the NBO calculations [26] were executed using NBO 3.1 program as implemented in the Gaussian 09W [20] package at the DFT/B3LYP level.

5. Results and Discussion

5.1. Molecular geometry

According to theoretical calculations the molecule 3AP has a nonplanar structure of C_1 symmetry consists of 11 atoms so it has 27 normal modes of internal vibrations. The optimized structure parameters of the compound were calculated by DFT/B3LYP level with 6-311G** basis set shown in **Table 1** in accordance with the atom numbering Scheme given in **Figure 1**.

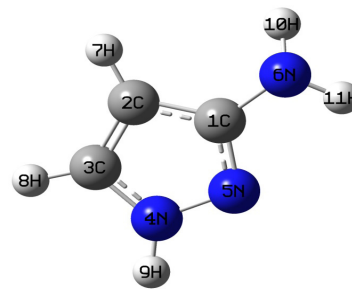


Figure 1: Molecular structure of 3-Amino Pyrazole along with numbering of atom.

Table 1: Optimized geometrical parameters of 3-amino Pyrazole obtained by B3LYP/ 6–311+G** density functional calculations.

Bond Length	Value(Å)	Bond Angle	Value(°)
C1-C2	1.422	C1-C2-C3	104.422
C2-C3	1.38	C2-C3-N4	106.622
C3-N4	1.354	C3-N4-N5	113.034
N4-N5	1.361	N4-N5-C1	104.01
N5-C1	1.333	N5-C1-C2	111.907
C2-H7	1.079	N5-N4-H9	118.848
C3-H8	1.08	C3-N4-H9	128.117
N4-H9	1.006	N4-C3-H8	121.955
C1-N6	1.398	C1-C2-H7	128.067
N6-H10	1.013	C2-C1-N6	127.307
N6-H11	1.013	N5-C1-N6	120.709
		C1-N6-H10	113.13
		C1-N6-H11	111.231
		H10-N6-H11	110.476
		C3-C2-H7	127.5
		C2-C3-H8	131.42

For numbering of atoms refer to **Figure 1**.

The C1-N6 bond length is a longer bond length of about 1.39 Å since these bonds play a bridge role between the carbon and amino group. The density functional calculation gives shortening of angles C3-C2-C1, N4-N5-C1, N4-C3-C2 and increasing of angles, C2-C1-N5 and N5-N4-C3 from 1100 exactly at the substitution and other parts of ring respectively. This asymmetry of angles reveals the conjugation with the Pyrazole ring and N-N group through a C-N double bond.

5.2. Vibrational analysis

The maximum number of active noticeable fundamental frequencies of a non-linear molecule (contains N atoms) is equal to $3N - 6$ excluding three translational and three rotational degrees of freedom. Accordingly 3AP has 27 normal modes of vibrations. The 27 normal modes of the title compound is distributed amongst the symmetry Species as

$$3N-6 = 15 \text{ (in - plane)} + 12 \text{ (out - of - plane)}$$

i.e., all the vibrations were active both in Raman scattering and infrared absorption. The A' vibrations are totally symmetric and

gives rise to polarized Raman lines whereas A^{''} vibrations are antisymmetric and gives rise to depolarized Raman lines.

For the entire assignment of fundamental vibrational modes of frequencies Normal Coordinate Analyses (NCA) were carried out to the compound 3AP. For this reason, the full set of 38 typical internal coordinates (containing 11 redundancies) of the compound was presented in **Table 2**.

Table 2: Definition of internal coordinates of 3-aminopyrazole.

No.(i)	Symbol	Type	Definition ^a
Stretching			
3-Jan	R _i	CN	C3-N4, C1-N5, C1-N6.
5-Apr	P _i	CC	C1-C2, C2-C3
7-Jun	Q _i	CH	C3-H8, C2-H7.
8	q _i	NH	N4-H9
10-Sep	q _i	NH	N6-H10, N6-H11.
11	T _i	NN	N4-N5.
In-Plane bending			
16-Dec	β _i	Ring1	C1-C2-C3, C2-C3-N4, C3-N4-N5, N4-N5-C1, N5-C1-C2.
17-20	σ _i	CCH	C1-C2-H7, C3-C2-H7, C2-C3-H8, N4-C3-H8.
21-22	δ _i	CCN	C2-C1-N6, N5-C1-N6.
23-24	α _i	CNH	C1-N6-H10, C1-N6-H11.
25	θ _i	HNH	H10-N6-H11.
26-27	α _i	NNH	N5-N4-H9, C3-N4-H9
Out-of-plane bending			
28	ω _i	CN	N6-C1-N5-C2.
29-30	π _i	CH	H7-C2-C1-C3, H8-C3-C2-N4.
31	ρ _i	NH	H9-N4-C3-N5.
Torsion			
32-36	τ _i	τ ring 1	C1-C2-C3-N4, C2-C3-N4-N5, C3-N4-N5-C1, N4-N5-C1-C2, N5-C1-C2-C3.
37-38	τ _i	τ NH2	C2-C1-N6-H10, N5-C1-N6-H11.

^aFor numbering of atom refer **Figure1**.

As of these, a non-redundant set of local symmetry coordinates were created by appropriate linear combinations of internal coordinates subsequent the recommendations of Fogarasi and co-workers [27] are reviewed in **Table 3**. The theoretically calculated DFT force fields were changed to the latter set of vibrational coordinates and used in all subsequent calculations.

The detailed fundamental vibrational modes of 3AP along with the calculated IR and Raman intensities and normal mode descriptions (characterized by PED) are reported in **Table 4**. By Selective scaling, the visual comparison of simulated IR and Raman spectra has shown in **Figures 2 and 3**, respectively.

Table 3: Definition of local-symmetry coordinates and the values of corresponding scale factors Used to correct the B3LYP/6-31G (d, p) (refined) force field of 3-Amino Pyrazole.

No.(i)	Symbol ^a	Definition ^b	Scale factors
Stretching			
3-Jan	v(C-N)	R1, R2, R3	0.922
5-Apr	v(C-C)	P4,P5	0.922
7-Jun	v(C-H)	Q6,Q7	0.911
8	v(N-H)	q8	0.911
9	v(NH2ss)	(q9-q10)/√2	0.934
10	v(NH2ass)	(q9+q10)/√2	0.934
11	v N-N	T11	0.944
In-Plane bending			
12	R2 bend1	β 1 2 + a (β 1 3 + β16)+b (β14-β15)	0.945
13	R2 bend2	(a - b) (β 1 3 - β16)+(1-a) (β15+β14)	0.945
14-15	bCH	(σ17- σ 18)/√2,(σ19- σ20)/√2	0.95
16	bCN	(δ21- δ22)/√2	0.964
17	NH2rock	(α 23- α 24)/√2	0.975
18	NH2twist	(α 23+ α 24)/√2	0.975
19	NH2sciss	(2θ25-α 23- α 24)/√2	0.975
20	bNH	(α 26- α 27)/√2	0.95
Out of plane bending			
21	ωCN	ω28	0.9744
22-23	ωCH	π29, π30.	0.9744
24	ωN-H	ρ31	0.9744
Torsion			
25	R2torsion1	τ34+b(τ36)+a(τ33+ τ35)	0.97
26	R2torsion2	(a-b)(τ33)+(1-a)(τ32- τ36)	0.975
27	τNH2	τ37+ τ38	0.974

a = cos 144° and b = cos 72°.

Abbreviations: v, stretching; b, in plane bending; ω, out of plane bending; τ, torsion, sym, symmetric deformation, asy, asymmetric deformation, twist, twisting, rock, rocking, sciss, scissoring, ss, symmetrical stretching, ass, asymmetrical stretching.

a These symbols are used for description of the normal modes by PED in Table 4.

b The internal coordinates used here are defined in Table 2.

s. no	Experimental (cm ⁻¹)		Scaled frequencies(cm ⁻¹)	Intensity		Characterization of normal modes with PED (%) ^{a,b}
	FT-IR	FT-Raman		I _R ^b	I _{RA} ^c	
1	-	-	3451	0.0405	55.9	υNH2as(100)
2	-	-	3404	0.0025	0.8	υNH2ss(100)
3	-	-	3327	0.483	46.1	υNH(99)
4	-	2995w	3071	0.00026	0.2	υCH(99)
5	2946w	2912s	2951	0.00991	65.5	υCH(99)
6	2360s	-	2361	0.00009	0.02	υCN(50),υCC(12),βNH2sw(11)
7	1734w	-	1734	0.0006	0.05	βNH2sci(59), βNH2tw(13),υCN(10)

Table 4: Detailed assignments of fundamental vibrations of 3-Amino Pyrazole by normal mode analysis based on SQM force field calculations using B3LYP/6-311G**.

8	1598s	-	1611	0.00198	0.11	β NH2sci(31), uCC(21), uCN(19)
9	-	-	1570	0.00415	0.17	uCN(44), β NH(37)
10	1507s	-	1492	0.823	13.2	uCC(43), uCN(20) β CH(13), β Rsym(11)
11	-	-	1443	0.0642	6.14	β CH(39), β NH(29), uCC(14)
12	-	-	1432	0.303	32.1	uCN(39), β CH(18), uNN(15), β NH2ro(14)
13	-	-	1358	0.0503	14.8	uCN(31), β NH2ro(29), β CH(12), uCC(12), β NH(10)
14	1272s	-	1291	0.0962	100	β CH(46), uCC(19), β NH2ro(13), uCN(12)
15	-	-	1202	0.0708	30.6	uCC(25), β CH(18), β Rasy(16), uNN(15), β NH2ro(10)
16	-	-	1190	0.0114	4.86	uNN(53), β Rasy(24), uCC(11)
17	-	-	1159	0.00227	0.93	β Rsym(62), β CH(14)
18	1122w	-	1106	0.026	26.9	ω CH(36), τ Rasy(24), ω CN(18), τ Rsym(17)
19	983s	-	984	0.00453	16.4	ω CH(41), τ Rsym(39), ω CN(14)
20	-	-	878	0.212	54.4	τ Rasy(42), τ Rsym(20), β NH2tw(7), ω CH(11)
21	-	-	827	0.00607	1.05	ω CH(60), β NH2tw(15)
22	-	-	713	0.0846	6	ω CH(32), τ Rasy(25), β Rasy(12)
23	668w	667vw	661	0.167	65.9	β NH2tw(48), uCN(23), τ Rasy(13)
24	-	-	607	0.0667	3.14	β CN(74)
25	-	-	500	0.00364	0.35	ω NH(69), τ Rsym(22)
26	-	332vw	376	0.584	53	ω CN(57), ω NH(13), τ Rsym(10)
27	-	-	250	0.301	69.5	τ NH2(82)

^aAbbreviations: ν , stretching; β , in plane bending; ω , out of plane bending; τ , torsion; ss, symmetrical stretching; as, asymmetrical stretching; tri, trigonal deformation; sym, symmetrical deformation; asy, asymmetric deformation, vs, very strong; s, strong; m, medium; w, weak; vw, very weak;

^bRelative absorption intensities normalized with highest peak absorption equal to 1.

^cRelative Raman intensities calculated by Eq. (1) and normalized to 100.

^dOnly PED contributions $\geq 10\%$ are listed.

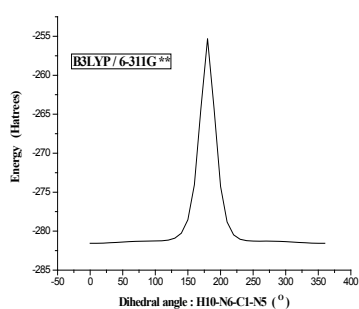


Figure 2: Potential energy surface scan for dihedral angle of 3-Amino Pyrazole.

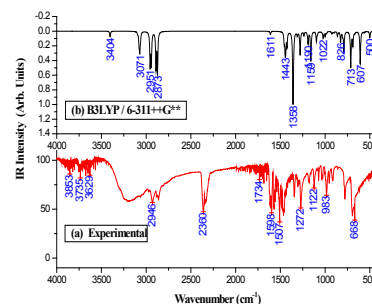


Figure 3: (a) Experimental, (b) Simulated FT-IR spectra of 3-amino pyrazole.

5.2.1. RMS values of frequencies were evaluated using the following expression:

$$RMS = \sqrt{\frac{1}{(n-1)} \sum_i^n (v_i^{calc} - v_i^{expt})^2}$$

The RMS error of the frequencies between the unscaled and experimental values was found to be 81.08 cm^{-1} . After scaling, the RMS error among the observed and scaled frequencies of 3AP by B3LYP/6-311+G** basis set is found to be 2.19 cm^{-1} .

5.2.2. C-H vibrations: The task of assigning carbon–hydrogen stretching mode is straight forward on the basis of the scaled ab initio predicted frequencies as well known “group frequencies”. The aromatic structure shows the presence of C-H stretching vibration in the Characteristic region of 3100–3000 cm^{-1} . In the present molecule, the expected C-H stretching vibrations observed at 3071 cm^{-1} scaled frequency and 2995 cm^{-1} in the FT-Raman spectrum are assigned to C2-H7 and C3-H8 Respectively. The in-plane C-H bending vibrations of benzene moreover its derivatives are examined in the region 1300–1000 cm^{-1} . The calculated frequency 1291 cm^{-1} is assigned to C-H in-plane bending vibration and this is in good agreement with the recorded FT-IR spectrum at 1272 cm^{-1} . The computed frequency at 826 cm^{-1} is allocated to C-H out-of-plane bending vibration. All the above assigned C-H vibrations are in good agreement with the previous literature [28].

5.2.3. N-H vibrations: The aromatic molecule containing an N-H group shows its stretching absorption in the region 3500–3200 cm^{-1} . The scaled frequency observed at 3327 cm^{-1} is assigned to N-H stretching vibration. The strong band observed at 1272 cm^{-1} in the FT-IR assigned to N-H in plane bending vibration.

5.2.4. Amino group vibrations: The frequencies of amino group appear around 3500–3300 cm^{-1} for NH2 stretching, 1700–1600 cm^{-1} for scissoring and 1150–900 cm^{-1} for rocking deformations. The antisymmetric and symmetric stretching modes of NH2 group scaled frequencies are found at 3451 cm^{-1} , 3404 cm^{-1} in 3AP. The weak IR bands for twisting NH2 modes of 3AP is identified at 668 cm^{-1} and very weak Raman bands for twisting NH2 mode is identified at 667 cm^{-1} . The Experimental bands are good

agreement with the scaled frequency 667 cm⁻¹.

5.2.5. C-C vibrations: The ring C=C and C-C stretching vibrations known as semicircle stretching usually occurs in the region 1625–650 cm⁻¹ [29-31]. Pyrazole ring has several bands of variable intensities in the range of 1530-1013 cm⁻¹ due to ring stretching vibration [32]. In the present study 1507 cm⁻¹ strong band observed in the FT-IR spectrum assigned to C-C vibration and another scaled frequency 1202 cm⁻¹ is assigned to another C-C vibration. The calculated frequencies have 25-43% contribution to the C-C stretching vibration from PED data. These vibrations may be assigned to C2=C3 and C1-C2 bonds.

5.2.6. C-N Vibrations: The task of C-N vibrations is a difficult because the mixing of vibrations is probable in the region. Through the force field calculations, the C-N vibrations are identified and assigned in this study. The position and intensity of the C-N stretching vibrations involving the nitrogen atom of the amino group will also help to identify the availability of the C-N vibrations.

6. Polarizability and Hyperpolarizability

Investigation of organic compounds possessing conjugated p-electron structures as well as large hyperpolarizability using infrared and Raman spectroscopy has been evolved as a focus of research [33]. In the present molecule the first hyperpolarizability β , dipole moment μ and polarizability α was calculated using HF/6-311G (d, p) basis set on the basis of the finite-field approach. The total static dipole moment μ , the mean polarizability α_0 , the anisotropy of the polarizability $\Delta\alpha$ and the mean first hyperpolarizability β_0 , using the x, y, z components are defined as

$$\mu = \mu_x^2 + \mu_y^2 + \mu_z^2 \quad (3)$$

$$\alpha_0 = \frac{\alpha_x + \alpha_y + \alpha_z}{3} \quad (4)$$

$$\Delta\alpha = 2 \frac{1}{2} [(\alpha_x - \alpha_y)^2 + (\alpha_y - \alpha_x)^2 + 6\alpha_x^2]^{1/2} \quad (5)$$

$$\beta = (\beta_x^2 + \beta_y^2 + \beta_z^2) \quad (6)$$

$$\beta_x = \beta_{xxx} + \beta_{xyy} + \beta_{xzz} \quad (7)$$

$$\beta_y = \beta_{yyy} + \beta_{xyx} + \beta_{yyz} \quad (8)$$

$$\beta_z = \beta_{zzz} + \beta_{xxz} + \beta_{yyz} \quad (9)$$

The HF/6-311G (d) calculated first hyperpolarizability of 3AP is $1.124122236 \times 10^{-30}$ esu and the dipole moment is 0.5625 Debye are shown in **Table 5**. The calculated first hyperpolarizability of

3AP is about 14 times greater than that of urea. The above results show that title compound is best material for NLO applications.

Table 5: Calculated all β components and β tot value of 3-Amino Pyrazole by HF/6-31G (d, p) method.

μ and α components	HF/6-31G(d, p)	β components	HF/6-31G(d, p)
μ_x	-0.0666798	β_{xxx}	94.6195367
μ_y	-0.3364337	β_{xyy}	-10.3364988
μ_z	0.6650308	β_{yyy}	-5.324604
$\mu(D)$	0.748264522	β_{yyy}	-0.1758175
α_{xx}	57.99183	β_{xzz}	61.5216615
α_{xy}	0.7563283	β_{xyx}	-1.5660475
α_{yy}	19.9031882	β_{yyz}	2.3058867
α_{xz}	3.7088761	β_{zzz}	-11.9460467
α_{yz}	0.4691956	β_{yzz}	-6.2480855
α_{zz}	50.4971563	β_{zzz}	39.4522665
α (esu)	6.342573×10^{-12} esu	β total (esu)	$1.124122236 \times 10^{-30}$ esu

7. NBO Analysis

The Natural Bond Orbital (NBO) computations were carried out so as to understand different second-order interactions amongst the filled orbital's of one subsystem and unfilled orbital's of a different subsystem, which is a measure of the delocalization or hyper conjugation. The interactive hyperconjugative energy is deduced from the second-order perturbation approach. For the molecule 3AP the orbital overlap between (C-C), (N-H), (C-H), (N-N) and (C-C), (N-H), (C-H), (N-N) antibond orbital are formed due to intramolecular hyper conjugative interactions. Moreover intramolecular charge transfer (ICT) happens which causes the stabilization of the system. For every donor (i) also acceptor (j), the stabilization energy E (2) joined through the delocalization i→j is predictable as

$$E^{(2)} = \Delta E_j = [q_i(F_{ij}^2)] [\epsilon_i - \epsilon_j] \quad (10)$$

Where q_i is the i^{th} donor orbital occupancy, ϵ_i , ϵ_j are diagonal elements and F_{ij} is the off diagonal elements of the NBO matrix.

The interactions among the lone-pair orbital's and their C-C and C-N filled orbital's are the large energetic repulsions. From the **Table 6**, the interaction among the lone pair N4 (1) and the antibond C2-C3 is seen to present the strongest stabilization, 44.34kcal/mol. This larger energy proves the hyper conjugation among the electron donating groups and the Pyrazole ring.

Table 6: Second order perturbation theory analysis of fock matrix in NBO basis for 3-Amino Pyrazole.

Donor(i)	Type	Ed/e	Acceptor(j)	Type	Ed/e	E(2) ^a (kJ mol ⁻¹)	E(i)-E(j) ^b (a.u)	f(i,j) ^c (a.u)
C1-C2	σ	1.97663	C2-C3	σ*	0.0093	1.69	1.25	0.041
	σ	1.97663	C3-H8	σ*	0.01355	5.17	1.14	0.069
	σ	1.97663	N6-H11	σ*	0.00804	1.9	1.14	0.042
C1-N5	σ	1.98471	C1-C2	σ*	0.02919	1.66	1.35	0.042
	σ	1.98471	C2-H7	σ*	0.01104	2.04	1.31	0.046
C1-N5	σ	1.8811	C2-C3	σ*	0.36541	11.49	0.32	0.058
	σ	1.8811	N6-H10	σ*	0.00717	1.23	0.76	0.028
C2-C3	σ	1.97548	C1-C2	σ*	0.02919	1.72	1.23	0.041
	σ	1.97548	C1-N6	σ*	0.02366	6.45	1.14	0.077
	σ	1.97548	N4-H9	σ*	0.01673	4.4	1.16	0.064
C2-C3	σ	1.8262	C1-N5	σ*	0.44246	27.91	0.28	0.084
C2-H7	σ	1.98384	C1-N5	σ*	0.01963	2.45	1.08	0.046
	σ	1.98384	C3-N4	σ*	0.0295	1.85	1.02	0.039
C3-N4	σ	1.9918	C2-H7	σ*	0.01104	3.17	1.32	0.058
C3-H8	σ	1.98504	C1-C2	σ*	0.02919	1.44	1.1	0.036
			N4-N5	σ*	0.01457	3.57	0.95	0.052
N4-N5	σ	1.98411	C1-N6	σ*	0.02366	6	1.27	0.078
			C3-H8	σ*	0.01355	2.27	1.3	0.048
N4-H9	σ	1.99106	C1-N5	σ*	0.01963	2.17	1.24	0.046
		1.99106	C2-C3	σ*	0.00913	1.43	1.28	0.038
N6-H10	σ	1.98338	C1-N5	σ*	0.01963	3.93	1.17	0.061
			C1-N5	σ*	0.44246	1.94	0.65	0.036
N6-H11	σ	1.98749	C1-C2	σ*	0.02919	5.38	1.16	0.071
LP								
N4(1)		1.58956	C1-N5	σ*	0.44246	24.99	0.28	0.076
			C2-C3	σ*	0.36541	44.34	0.29	0.102
N5(1)		1.94369	C1-C2	σ*	0.02919	6.38	0.93	0.069
			C3-N4	σ*	0.02495	6.81	0.88	0.07
N6(1)		1.87773	C1-N5	σ*	0.44246	26.48	0.32	0.089

^a E(2) means energy of hyper conjugative interaction (stabilization energy).

^b Energy difference between donor and acceptor i and j NBO orbital's.

^c F(i, j) is the Fock matrix element between i and j NBO orbital's.

8. HOMO-LUMO Energy Gap and UV-Vis Spectrum

Several organic molecules having conjugated π electron are expressed by huge values of first order hyperpolarizabilities are investigated by means of vibrational spectroscopy [34]. The molecules are described by a small highest occupied molecular orbital-lowest unoccupied molecular orbital separation. The HOMO and LUMO topologies gives definite overlap of two orbital's in the middle region of the π -conjugated systems, this is a requirement to allow an efficient charge transfer transition. The HOMO-LUMO energy gap determined by B3LYP/6-311++G** method are shown in Table 7. The HOMO-LUMO gap has been calculated as 6.36284143eV and is shown in figure 5. The Visualization of the molecular orbital's [MO: 15-MO: 30] of 3-Amino Pyrazole under C1 symmetry is shown in figure 6. The experimental UV-Vis spectrum is shown in figure 7 and value of λ maxis 257.65 nm.

Table 7: The calculated quantum chemical parameters for 3-amino pyrazole obtained by B3LYP/6-31 1G ** calculations.

Property	3-aminopyrazole
Total energy (a.u)	-1
EHOMO(eV)	-5.446089
ELUMO(eV)	0.916752
EHOMO-ELUMO(eV)	-6.362841
Electronegativity (χ)eV	2.264668
Chemical hardness(η)eV	-3.18142
Electrofilicity index (ω) eV	-0.806043
Global Softness (σ)eV	-0.314324
Total energy change(Δ ET) eV	0.795355
Dipole moment(D)	0.5625

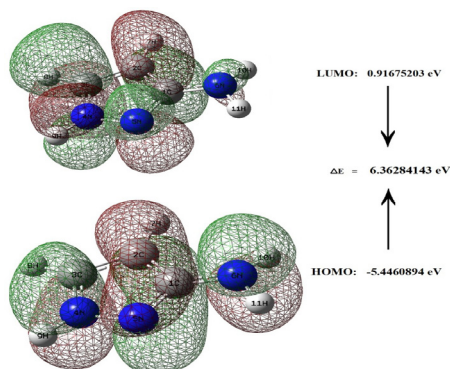


Figure 5: The atomic orbital components of the frontier molecular orbital (HOMO-MO: 22, LUMO-MO: 23) of 3-Amino Pyrazole.

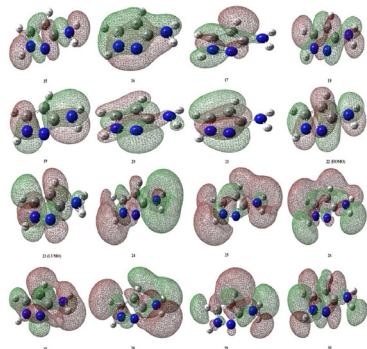


Figure 6: Visualization of the molecular orbitals [MO: 15-MO: 30] of 3-Aminopyrazole under C1 symmetry: HOMO-MO: 22 and LUMO-MO: 23.

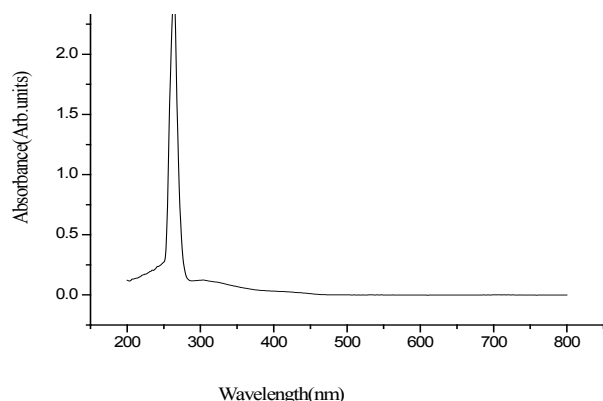


Figure 7: Experimental UV/Vis spectra of 3-Amino pyrazole.

9. Thermo Dynamic Properties

On the basis of vibrational analyses and statistical thermodynamics, the standard thermodynamic functions such as heat capacity, internal energy, entropy and enthalpy are calculated and are listed in Table 8. As observed from **Table 8**, the values of CP, CV, U, H and S all increase with the increase of temperature from 50 to 500 K, which is attributed to the enhancement of the molecular vibration as the temperature increases.

10. Molecular Electrostatic Potential

The Molecular Electrostatic Potential (MEP) is determined over the entire accessible surface of the molecules (this corresponds with the Van der Waals contact surface). The positive electrostatic potential regions indicate an excess of positive charge, while the negative potential regions indicate areas with an excess of negative charge. The MEP of 3-amino pyrazole is obtained based on the DFT optimized result and shown in **Figure 8**.

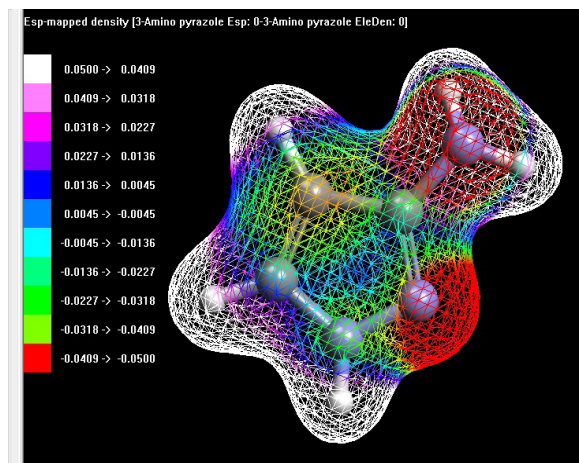


Figure 8: B3LYP/6-311++G** calculated 3D molecular electrostatic potential maps of 3-amino pyrazole.

Table 8: Thermo dynamical parameters of 3-Amino Pyrazole.

temperature (K)	CV (J/K/mol)	CP (J/K/mol)	U (kJ/mol)	H (kJ/mol)	S (J/K/mol)	G (kJ/mol)
50	63.226	73.8415	552.495	549.795	302.459	541.177
100	97.029	105.344	559.434	560.265	353.094	524.956
150	130.766	139.08	565.114	566.362	402.071	506.051
200	178.24	176.555	572.575	574.238	447.13	484.812
250	218.21	218.525	582.97	583.029	480.784	441.32
300	239.433	257.787	596.389	596.883	543.826	445.732
350	289.076	294.391	616.786	629.716	586.324	417.975
400	332.877	341.291	630.16	635.345	626.175	368.129
450	354.781	373.986	649.089	643.793	689.123	356.194
500	379.888	389.463	644.476	666.823	688.903	314.287

References

- Tewari AK, Mishra A. Synthesis and anti-inflammatory activities of N4, N5-disubstituted-3-methyl- H-pyrazolo[3,4-c]pyridazines. *Bioorg Med Chem.* 2001;9(3):715-8.
- Xia Y, Dong ZW, Zhao BX, Ge X, Meng N, Shin DS, et al. Synthesis and structure-activity relationships of novel 1-arylmethyl-3-aryl-1H-pyrazole-5-carbohydrazide derivatives as potential agents against A549 lung cancer cells. *Bioorg Med Chem.* 2007;15(22):6893-9.
- Michon V, du Penhoat CH, Tombret F, Gillardin JM, Lepage F, Berthon L. Preparation, structural analysis and anticonvulsant activity of 3- and 5-aminopyrazole N-benzoyl derivatives. *Eur J Med Chem.* 1995;30(2):147-55.
- Bailey DM, Hansen PE, Hlavac AG, Baizman ER, Pearl J, DeFelice AF, et al. 3, 4-Diphenyl-1H-pyrazole-1-propanamine antidepressants. *Med Chem.* 1985;28(2):256-60.
- Sridhar R, Perumal PT, Etti S, Shanmugam G, Ponnuswamy MN, Prabavathy VR, et al. Design, synthesis and anti-microbial activity of 1H-pyrazolecarboxylates. *Bioorg Med Chem Lett.* 2004;14(24):6035-40.
- Kumar S, Meenakshi, Kumar S, Kumar P. Synthesis and antimicrobial activity of some (3-phenyl-5-(1-phenyl-3-aryl-1H-pyrazol-4-yl)-4,5-

- dihydro-1H-pyrazol-1-yl)(pyridin-4-yl) methanones: new derivatives of 1,3,5-trisubstitutedpyrazolines. *Med Chem Res.* 2013;22(1):433-9.
7. Moura NM, Nunez C, Santos SM, Faustino MA, Cavaleiro JA, Neves MG, et al. Synthesis, Spectroscopy Studies, and Theoretical Calculations of New Fluorescent Probes Based on Pyrazole Containing Porphyrins for Zn(II), Cd(II), and Hg(II) Optical Detection. *Inorg Chem.* 2014;53(12):6149-58.
8. Burschka J, Dualeh A, Kessler F, Baranoff E, Cevey-Ha N, Yi C, et al. Tris(2-(1H-pyrazol-1-yl)pyridine)cobalt(III) as p-Type Dopant for Organic Semiconductors and Its Application in Highly Efficient Solid-State Dye-Sensitized Solar Cells. *J Am Chem Soc.* 2011;133(45):18042-5.
9. Grazul M, Besic-Gyenge E, Maake C, Ciolkowski M, Czyz M, Sigel RKO, et al. Synthesis, Physico-Chemical Properties and Biological Analysis of Newly Obtained Copper(II) Complexes with Pyrazole Derivatives. *J Inorg Biochem.* 2014;135:68-76.
10. Ovejero P, Asensio E, Heras JV, Campo JA, Cano M, Torres MR, et al. Silver-pyrazole complexes as hybrid multifunctional materials with metallomesogenic and photoluminescent behaviour. *Dalton Trans.* 2013;42(6): 2107-20.
11. Jing Xiong, Wei Liu, Yong Wang, Long Cui, Yi-Zhi Li, Jing-Lin Zuo. Tricarbonyl Mono- and Dinuclear Rhenium (I) Complexes with Redox-Active Bis(pyrazole)-Tetrathiafulvalene Ligands: Syntheses, Crystal Structures, and Properties. *Organometallics.* 2012;31(10):3938-46.
12. Erdemir S, Malkondu S. A novel "turn on" fluorescent sensor based on hydroxyl triphenylamine for Zn²⁺ and Cd²⁺ ions in MeCN. *Sens Actuators B Chem.* 2013;188:1225-9.
13. Banerjee, Samanta PN, Das KK, Ababei R, Kalisz M, Girard A, et al. Air oxygenation chemistry of 4-TBC catalyzed by chloro bridged dinuclear copper(II) complexes of pyrazole based tridentate ligands: synthesis, structure, magnetic and computational studies. *Dalton Trans.* 2013;42(5):1879-92.
14. de Leon, Guerrero M, Garcia-Anton J, Ros J, Font-Bardia M, Pons J. Study of new metallomacrocyclic Pd(II) complexes based on hybrid pyrazole sulfoxide/sulfone ligands and their contribution to supramolecular networks. *Cryst Eng Comm.* 2013;15(9):1762-71.
15. Majoube M, Michel. Vibrational spectra of pyrazole and deuterium-substituted analogues. *J Raman Spectrosc.* 1989;20(1):49-60.
16. Majoube M. The .nu. NH mode and its coupling with the .gamma. NH mode for vapor pyrazole and its C-deuterium substituted analogues. *J Phys Chem.* 1988;92(9):2407-10.
17. Tabacik V, Sportouch S. CH stretching vibrations of pyrazole and of its deuterated species. Anharmonicity of modes and molecular pseudo-symmetry. *J Raman Spectrosc.* 1978;7(2):61-6.
18. Meryem Evecen, HasanTanak, FeyzaTinmaz, NecmiDege, IlhanOzerIlhan. Experimental (XRD, IR and NMR) and theoretical investigations on 1-(2-nitrobenzoyl) 3, 5-bis(4-methoxyphenyl)-4,5-dihydro-1H-pyrazole. *Mol Struct.* 2016;1126:117-26.
19. Krishnakumar V, Jayamani N, Mathammal R. Molecular structure, vibrational spectral studies of pyrazole and 3,5-dimethyl pyrazole based on density functional calculations. *Spectrochim Acta A Mol Biomol Spectrosc.* 2011;79(5):1959-68.
20. Frisch MJ, Trucks GW, Schlegel HB, Scuseria GE, Robb MA, Cheeseman JR, G. Scalmani, V. Barone, B. Mennucci, G.A. Petersson, H. Nakatsuji, M. Caricato, X. Li, H.P. Hratchian, A.F. Izmaylov, J. Bloino, G. Zheng, J.L. Sonnenberg, M. Hada, M. Ehara, K. Toyota, R. Fukuda, J. Hasegawa, M. Ishida, T. Nakajima, Y. Honda, O. Kitao, H. Nakai, T. Vreven, J.A. Montgomery Jr., J.E. Peralta, F. Ogliaro, M. Bearpark, J.J. Heyd, E. Brothers, K.N. Kudin, V.N. Staroverov, R. Kobayashi, J. Normand, K. Raghavachari, A. Rendell, J.C. Burant, S.S. Iyengar, J. Tomasi, M. Cossi, N. Rega, J.M. Millam, M. Klene, J.E. Knox, J.B. Cross, V. Bakken, C. Adamo, J. Jaramillo, R. Gomperts, R.E. Stratmann, O. Yazyev, A.J. Austin, R. Cammi, C. Pomelli, J.W. Ochterski, R.L. Martin, K. Morokuma, V.G. Zakrzewski, G.A. Voth, P. Salvador, J.J. Dannenberg, S. Dapprich, A.D. Daniels, E.O. Farkas, J.B. Foresman, J.V. Ortiz, J. Cioslowski, D.J. Fox, Gaussian, Inc, 2009. Wallingford CT.
21. G. Rauhut, P. Pulay. Transferable Scaling Factors for Density Functional Derived Vibrational Force Fields. *J Phys Chem.* 1995;99(10):3093-100.
22. Pulay P, Fogarasi G, Pongor G, James Boggs E, Vargha A. Combination of theoretical ab initio and experimental information to obtain reliable harmonic force constants. Scaled quantum mechanical (QM) force fields for glyoxal, acrolein, butadiene, formaldehyde, and ethylene. *J Am Chem Soc.* 1983;105(24):7037-47.
23. Fogarasi G, Pulay P, Durig JR. Chapter 3, Vibrational Spectra and Structure. Elsevier Amsterdam. 1985;14(125).
24. T. Sundius. Molvib - A flexible program for force field calculations. *J Mol Struct.* 1990;218:321-6.
25. T. Sundius. Scaling of ab initio force fields by MOLVIB. *Vibr Spectrosc.* 2002;29(1-2):89-95.
26. Glendering ED, Reed AE, Carpenter JE, Weinhold F. NBO Version 3.1. TCI, University of Wisconsin, Madison. 1998.
27. Fogarasi G, Zhou X, Taylor PW, Pulay P. The calculation of ab initio molecular geometries: efficient optimization by natural internal coordinates and empirical correction by offset forces. *J Am Chem Soc.* 1992;114(21):8191-201.

28. Swaminathan J, Ramalingam M, Sundaraganesan N. Molecular structure and vibrational spectra of 3-amino-5-hydroxypyrazole by density functional method. *Spectrochim Acta A Mol Biomol Spectrosc.* 2009;71(5):1776-82.
29. Krishna kumar V, Prabhavathy N, Muthunatesan N. Structure and vibrational frequencies of 1-naphthaldehyde based on density functional theory calculations. *Spectrochim Acta A.* 2008;69(2):528-33.
30. Rastogi K, Palafox MA, Tanwar RP, Mittal L. 3,5-Difluorobenzonitrile: ab initio calculations, FTIR and Raman spectra. *Spectrochim Acta A Mol Biomol Spectrosc.* 2002;58(9):1987-94.
31. Altun K, Golcuk M, Kumru. Structure and vibrational spectra of p-methylaniline: Hartree-Fock, MP2 and density functional theory studies. *J Mol Struct (Theochem).* 2003;637(1-3):155-69.
32. Rostkowska H, Nowak MJ, Lapinski L, Bertner M, Kullikowski T, Ces A, et al. Infrared spectra of 2-thiocytosine and 5-fluoro-2-thiocytosine; experimental and ab initio studies. *Spectrochim Acta A Mol Spectrosc.* 1993;49(4):551-65.
33. Tommasini M, Castiglioni C, Del Zoppo M, Zerbi G. Relationship between infrared and Raman intensities in molecules with polarized π electrons. *J Mol Struct.* 1999;480-1:179-88.
34. Vijayakumar T, Joe IH, Jayakumar VS. Efficient π electrons delocalization in prospective push-pull non-linear optical chromophore 4-[N,N-dimethylamino]-4'-nitro stilbene (DANS): A vibrational spectroscopic study. *Chem Phys.* 2008;343(1):83-99.